Supporting Information

Plasmon-assisted mode selection lasing in a lanthanide-based microcavity

Lei Guo[1], Min Ji[1], Bowen Kang[1], Min Zhang[1], Xin Xie[1], Zihao Wu[1], Huan Chen[1*], Volker Deckert[2], Zhenglong Zhang[1*]

[1]School of Physics and Information Technology, Shaanxi Normal University, Xi'an, China

[2]Leibniz Institute of Photonic Technology, Friedrich-Schiller University, Jena, Germany

CONTENTS:

1. Materials and methods
2. Size distribution diagram of upconversion nanoparticles
3. FWHM and Q factors of microlaser
4. Emission polarization fluorescence spectra
5. Excited power density-dependent upconversion luminescence
6. Quality factors of microcavity under different excitation power densities
7. Fluorescence lifetime of UCNPs and laser lifetime of microcavity
8. Charge distribution of isolated dipole sources on the silver microplate
9. Fluorescence spectrum of UCNPs@SiO_2 microsphere
10. Lasing peaks in different bands of microcavity
11. Fluorescence emission spectra of SiO_2@UCNPs microsphere on the different substrates
12. Simulated electric field diagram of microcavity on the silver microplate
13. WGM lasing excited by SPPs of different directions remotely
14. Calculated electric field distribution for a two-sphere system
15. The thickness distribution of the SiO_2 core and UC shell
16. The intensity ratio between whispering gallery TE mode and TM mode
17. The intensity ratio of two splitting peaks

1. Materials and methods

Fabrication of the Plasmon upconverting microlaser

The upconversion nanoparticles were synthesized by high-temperature thermal decomposition. In short, 2 mmol precursor ($Y(C_2H_3O_2)_3$, $Yb(C_2H_3O_2)_3$, $Tm(C_2H_3O_2)_3$) was added with 12 mL oleic acid (OA, technical grade, Sigma Aldrich) and 30 mL octadecene (ODE, Technical grade, Sigma Aldrich) blend in a three-necked flask. To obtain a uniform liquid mixture, the solution was heated to 160 ℃ under intense stirring in an argon atmosphere and held for 60 minutes. It was then cooled to room temperature. Afterwards, 10ml methanol solution containing 2.5 mmol NaOH and 20 ml methanol solution containing 4 mmol NH_4F were slowly injected into the mixed solution in the flask, stirred at room temperature for 60 min, then slowly heated to remove the methanol, vacuumized at 108 ℃ for 40 min. The solution was then allowed to cool to room temperature and centrifuged with ethanol and cyclohexane three times. Finally, the sample was dissolved in cyclohexane and stored for further use.

Single crystal silver micron triangles were synthesized by a wet chemical method. Dissolve 1 m metol and hydrazine mixture in 10 ml ultra-pure water, then add 10 ml 0.03 m $AgNO_3$. After the drip is finished, wash it several times with ultra-pure water and alcohol. Silver nitrate ($AgNO_3$), methanol, and hydrazine were purchased from Sigma Aldrich.

The upconversion microcavity composed of silica microspheres and up-conversion nanoparticles was realized by the bottom-up preparation method. The diluted silica microsphere solution was deposited on the glass substrate, and then the diluted upconversion nanoparticle solution was spin-coated on the prepared substrate for 45 seconds at the speed of 1200 rpm/min. The surface of the silica microsphere was coated with uniform and dense upconversion nanoparticle films. Then, to prepare the plasmon upconversion microcavity, the diluted silver microplate solution was deposited on the silicon substrate and the upconversion microcavity on the glass substrate was transferred to the silver microplate on the silicon substrate by micromanipulation technique.

Characterizations and measurements

The morphology of upconversion nanoparticles was characterized by JEOL-JEM 2100F transmission electron microscope (TEM) at 200 kV accelerated voltage. Scanning electron microscope (SEM) images were obtained by FEI-Nova SEM 450 (Hillsboro, OR, USA) at 10 kV, and fluorescence spectrum measurements were performed using a homemade confocal upconversion fluorescence microscopic system. The samples were excited by a continuous wave laser (Cobolt 06-mrd-975)

with a wavelength of 976 nm. In situ and remote upconversion fluorescence spectra were collected by ×100 and 0.9-NA microscopes, and then by a short-pass fluorescence filter at 850 nm and analyzed by spectrometers (Horiba iHR550 and Renishaw inVia Raman microscope). Optical images were acquired with a 100× objective lens (NA = 0.9, Olympus).

2. Size distribution diagram of upconversion nanoparticles.

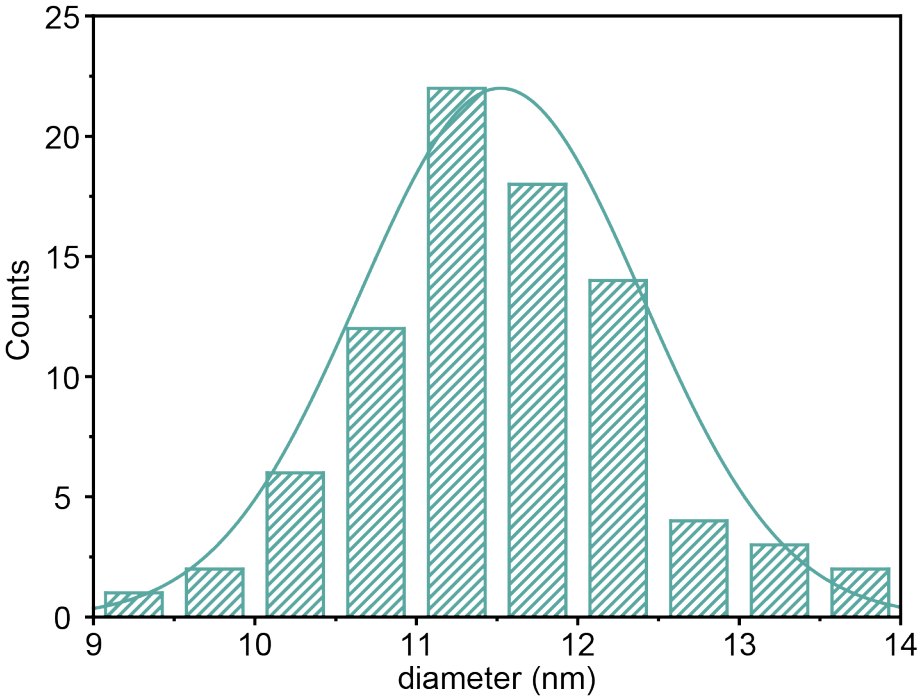

Figure S1. Size distribution diagram of the as synthesized upconversion nanoparticles, which shows the size uniformity of the nanoparticles.

3. FWHM and Q factors of microlaser.

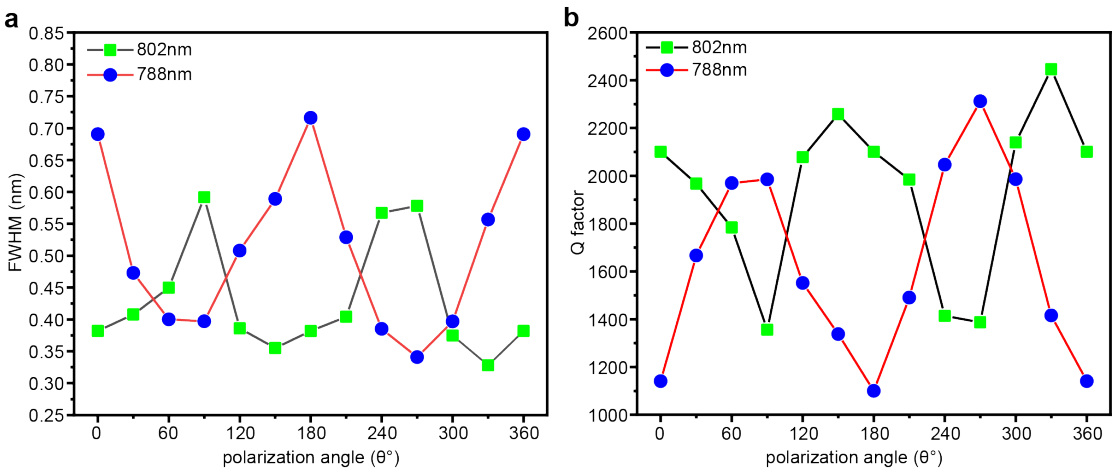

Figure S2. FWHM (a) and Q factor (b) of a single microlaser as a function of polarizer rotation angles θ.

4. Emission polarization fluorescence spectra.

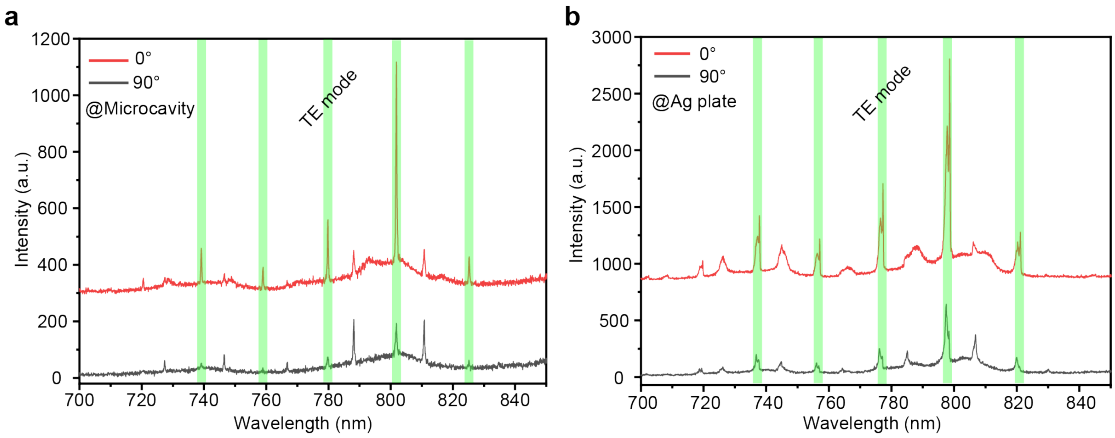

Figure S3. Emission polarization fluorescence spectra of the upconversion microcavity on the glass substrate and the silver microplate, respectively, when the polarizer is located at 0 degrees (a) and 90 degrees (b).

5. Excited power density dependent upconversion luminescence.

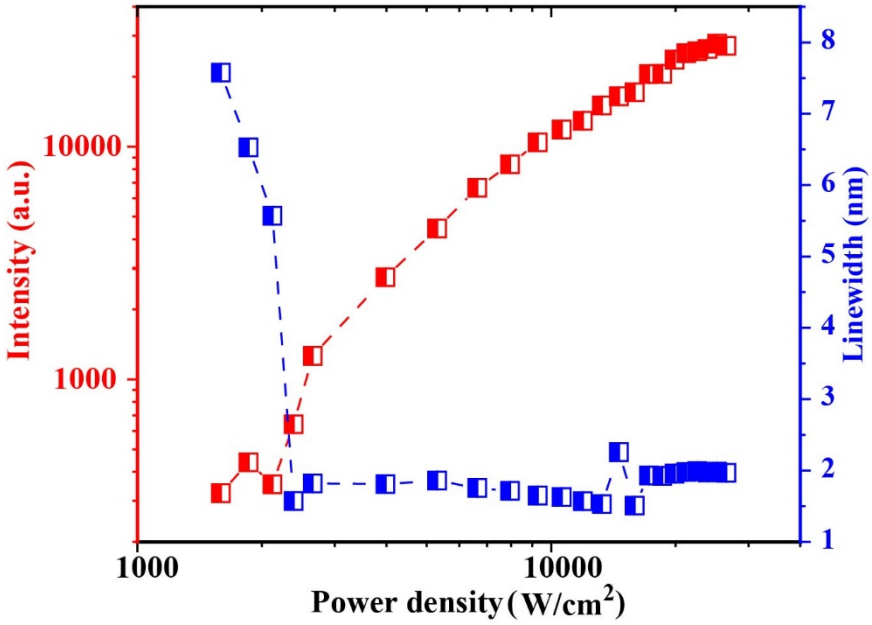

Figure S4. The excitation power dependence diagram when the upconversion microcavity is located on the silver microplate, we can see that with the increase of excitation power, the integrated emission intensity of the shape peaks exhibits a steeper increasing slope, and the full width at half maximum (FWHM) narrows substantially, demonstrating lasing behavior in the upconversion microcavity on the silver microplate.

6. Quality factors of microcavity under different excitation power densities.

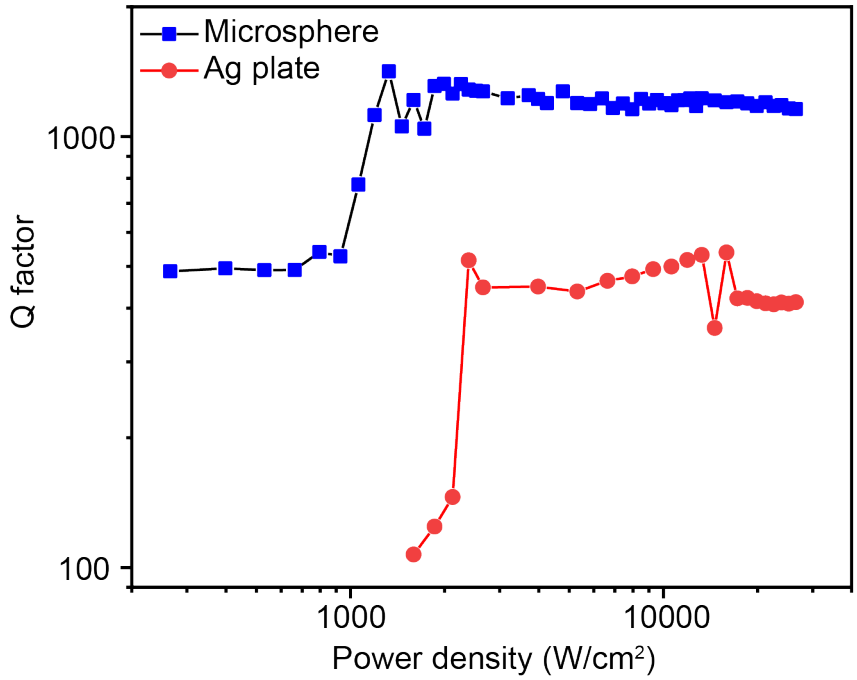

Figure S5. The change of quality factor of the upconversion microcavity on a glass substrate and a silver microplate under different excitation power densities.

7. Fluorescence lifetime of UCNPs and laser lifetime of microcavity.

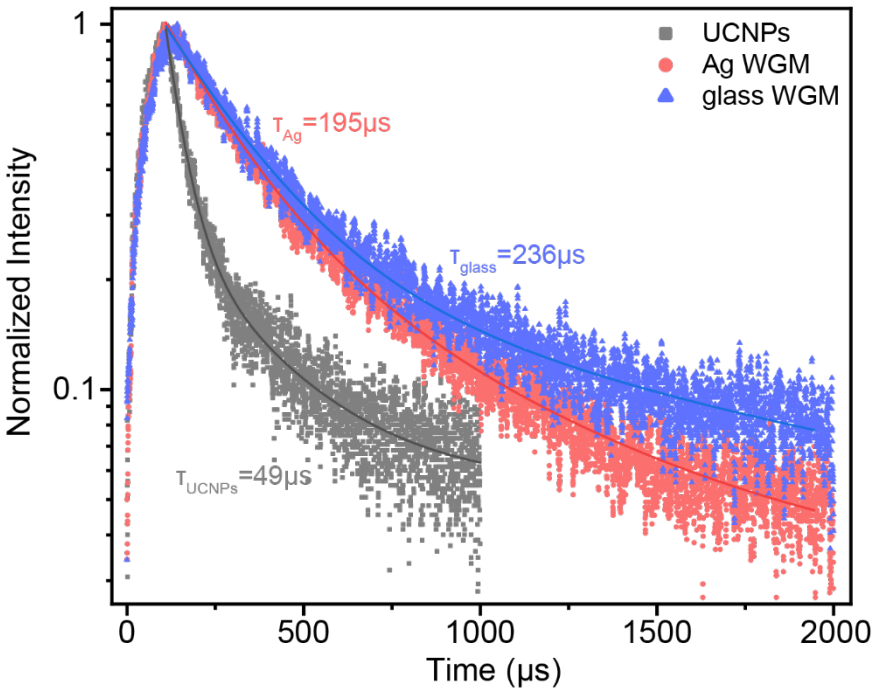

Figure S6. Fluorescence lifetime of UCNPs and lasing lifetime of microcavity on a glass substrate and a silver microplate.

8. Charge distribution of isolated dipole sources on the silver microplate.

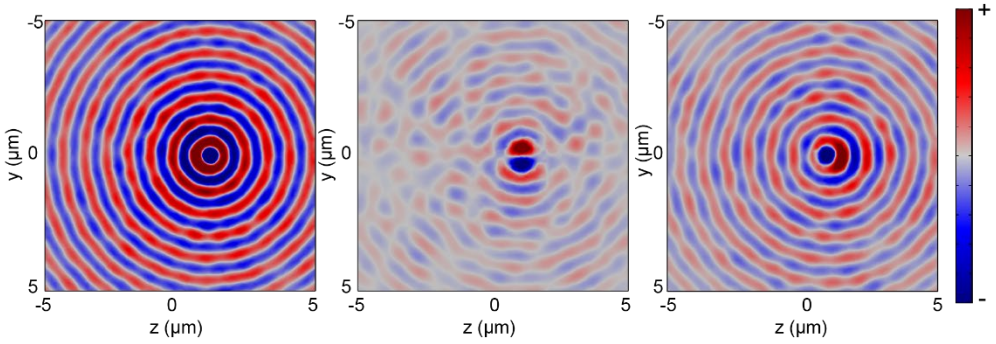

Figure S7. The charge distribution when a single dipole is placed on a silver microplate.

9. Fluorescence spectrum of UCNPs@SiO_2 microsphere.

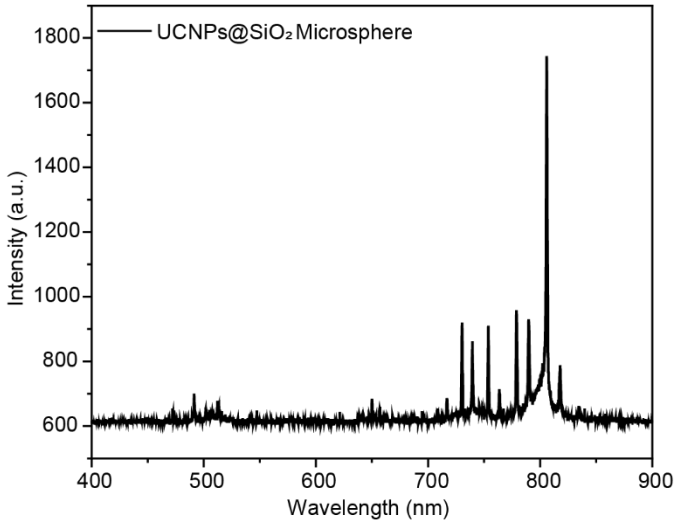

Figure S8. Fluorescence spectrum of UCNPs@SiO_2 microsphere.

10. Lasing peaks in different bands of microcavity.

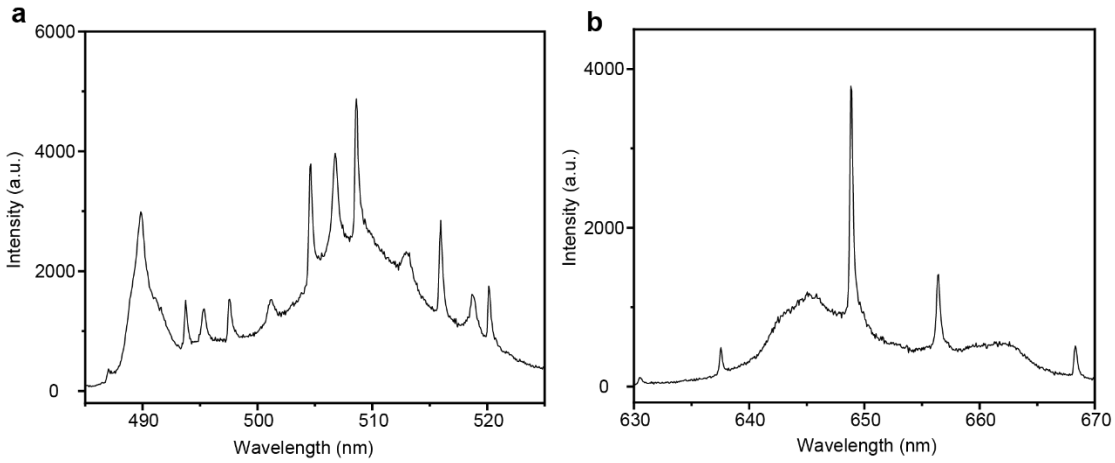

Figure S9. Fluorescence emission spectra of a SiO_2@UCNPs microsphere at 490–520nm (a) and 630–670nm (b) wave band.

11. Fluorescence emission spectra of SiO_2@UCNPs microsphere on the different substrates.

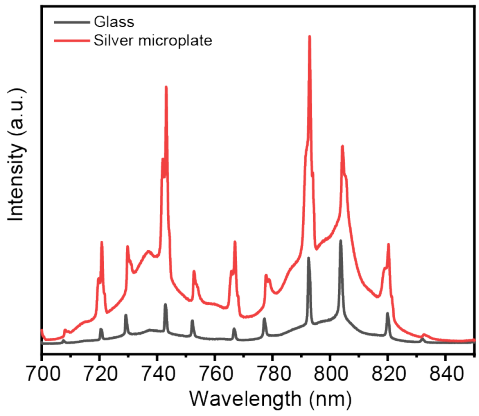

Figure S10. Fluorescence emission spectra of SiO_2@UCNPs microsphere on the glass substrate and silver microplate.

12. Simulated electric field diagram of microcavity on the silver microplate.

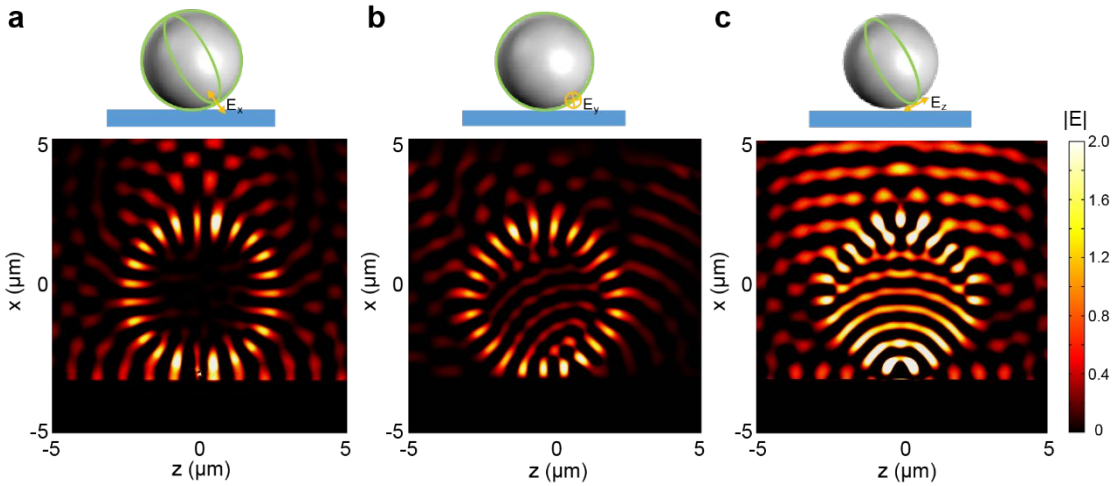

Figure S11. Schematic diagram of microcavity on silver microplate excited by a dipole with different electric field orientation (a) E_x, (b) E_y, (c) E_z and simulated electric field profile corresponding to the x-z plane.

13. WGM lasing excited by SPPs of different directions remotely.

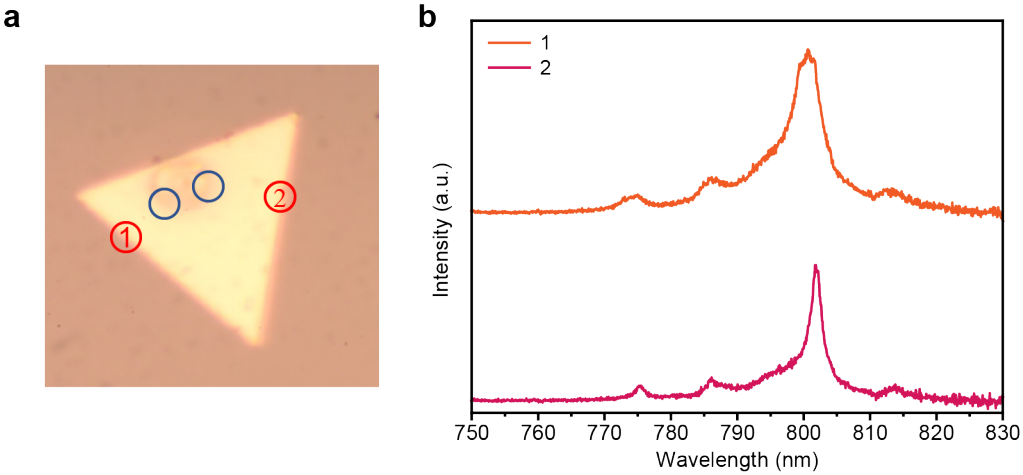

Figure S12. (a) Microscope image of WGM excited by SPP remotely (excitation positions at red circles 1 and 2, collection positions corresponding to the left and right blue circles.) (b) Emission spectrum of microcavity on the silver microplate when the laser polarization direction is perpendicular to the edge of the silver microplate.

14. Calculated electric field distribution for a two-sphere system.

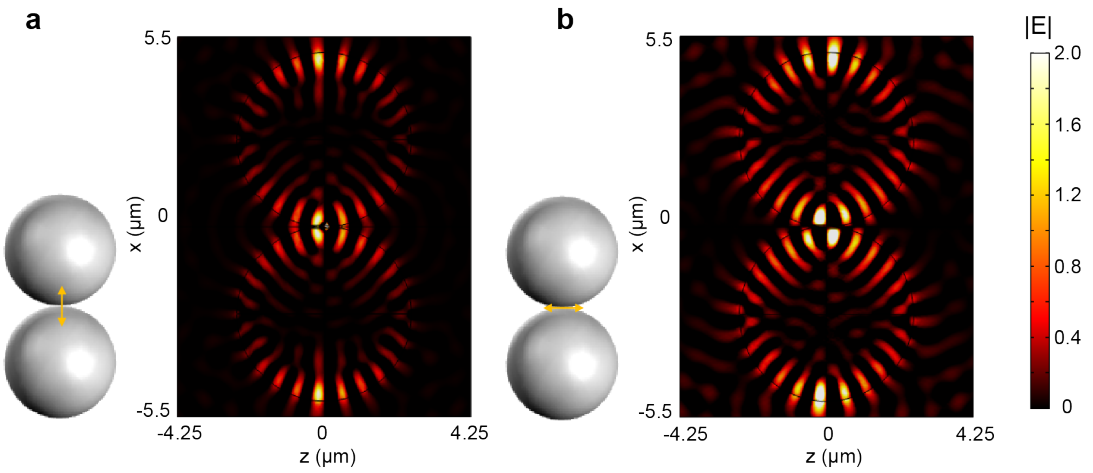

Figure S13. The model system, two-sphere in contact, considered to represent the microsphere on a mirror. Calculated electric field distribution for a two-sphere system by placing (a) single dipole along the x-axis, and (b) single dipole along the z-axis.

15. The thickness distribution of the SiO_2 core and UC shell.

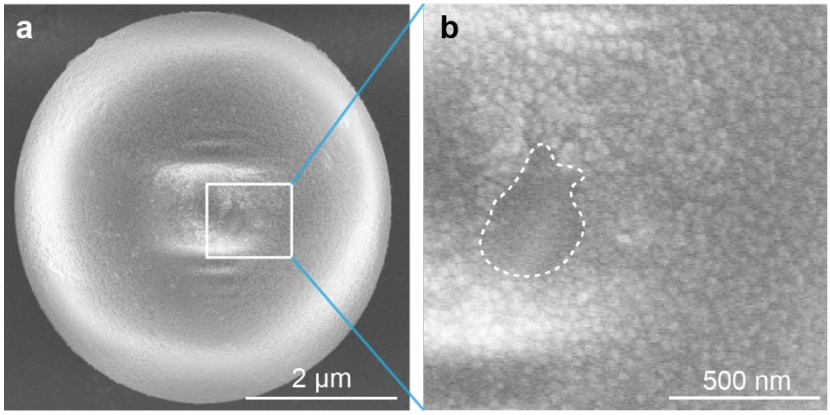

Figure S14. SEM images of (a) UCNPs-coated SiO_2 microsphere, (b) a partial enlargement view of the white box in a, the white dotted line is the surface of the silica microsphere without UCNPs.

16. The intensity ratio between whispering gallery TE mode and TM mode.

Experiment (I_{TE}/I_{TM})			Simulation (I_{TE}/I_{TM})		
Ag	glass	Ag/glass	Ag	glass	Ag/glass
1.42	1.39	1.02	1.51	1.17	1.29
2.19	1.04	2.11	1,35	0.99	1.36
2.03	0.93	2.18	1.56	0.99	1.58
4.07	2.98	1.37	1.45	1.06	1.37

Table S1. Intensity ratio table of TE, TM mode lasing on silver microplate and glass substrate on experiment and simulation.

17. The intensity ratio of two splitting peaks.

	Left	Right	Ratio (R/L)
	2465.41	2993.63	1.21
0°	1374.1	1964.19	1.43
90°	642.618	404.66	0.63
	2016.718	2368.85	1.17

Table S2. Comparison table of the intensity values of the two splitting peaks when the polarizer is not added and when the polarization angle is 0° and 90°.